Dalton Transactions

PAPER

View Article Online
View Journal

Cite this: DOI: 10.1039/c5dt03883a

Zebra reaction or the recipe for the synthesis of heterodimeric zinc complexes†

D. Jędrzkiewicz, J. Ejfler,* Ł. John and S. Szafert

Received 5th October 2015,
Accepted 13th November 2015

DOI: 10.1039/c5dt03883a

www.rsc.org/dalton

A series of asymmetric heterodimeric zinc complexes have been synthesized in a direct reaction between conformationally flexible chiral/achiral homodimers. The cooperative activity of steric factors and coordination codes resulted in an intriguing chiral self-sorting process. Herein, we are reporting our recent exploration of the first example of such a type of reaction.

Introduction

Zinc complexes with functionalized monoanionic chelating amino/imino-phenols, *i.e.* Schiff-base type ligands, have found widespread applications in coordination chemistry, biological systems and catalysis.[1] The structural motif of the coordinating ligand for the selected application requires a conformationally rigid ligand framework, employed for the stabilization of the metal center, or on the contrary, flexibility of the ligand is the priority to achieve the desired molecular architecture for the metal complexes of an interesting reaction. Therefore, the precise design of ligands with optimal conformational freedom is of course the first stage of the planned synthetic strategy but unfortunately sometimes undoable in practice. Instead, unplanned and unexpected reactivity of even tedious, well-known complexes could constitute a valuable support for sophisticated synthesis.

Well-defined alkyl zinc complexes with N, O-donor ligands confirmed by X-ray analysis are known and usually present monomeric or dimeric structures.[2,3] Recently, we have explored the combination of functionalized aminophenol ligands with $ZnEt_2$ for the targeted synthesis of homodimeric complexes. The experimental data as well as the theoretical DFT calculations indicate that aminophenolate ligands with a free *ortho*-position of the phenol ring prefer the formation of dimeric alkyl zinc complexes, irrespective of the substrates' molar ratio.[4a]

Here we are reporting a new type of substrate for the new synthetic strategy tailored for the acquisition of heterodimeric zinc complexes. The synthesis of zinc dimers containing metal centers bearing different ancillary ligands is possible in one pot, by means of a simple and efficient procedure with the application of the classical zinc aminophenolates.

Department of Chemistry, University of Wrocław, 14 F. Joliot-Curie, 50-383 Wrocław, Poland. E-mail: jolanta.ejfler@chem.uni.wroc.pl; Tel: +48 (71) 375 7310

† Electronic supplementary information (ESI) available: ^{1}H, ^{13}C, NOESY spectra, X-ray experimental data and refinement, DFT and DOSY calculations. CCDC 1046690, 1427070, 1046689, 1427071 and 1434203. For ESI and crystallographic data in CIF or other electronic format see DOI: 10.1039/c5dt03883a

Experimental

General materials, methods and procedures

All reactions and operations were performed under an inert atmosphere of N_2, while using a glove-box (MBraun) or standard Schlenk techniques. Reagents were purified using standard methods: toluene, distilled from Na; hexanes, distilled from Na; methanol, distilled from Mg; C_6D_6, distilled from CaH_2. $ZnEt_2$ (1.0 M solution in hexanes), *N*-α-dimethylbenzylamine, *N*-methylcyclohexylamine, *N*-dimethylamine (2 M solution in MeOH), formaldehyde (37% solution in H_2O), and 4-*tert*-butylphenol were purchased from Aldrich and used as received. ^{1}H and ^{13}C NMR spectra were collected at the temperature range from 233 to 333 K, while using Bruker ESP 300E or 500 MHz spectrometers. Chemical shifts are reported in parts per million and referenced to residual protons in deuterated solvents.

Syntheses

***N*-[Methyl(2-hydroxy-5-*tert*-butylphenyl)]-*N*-methyl-*N*-(1-phenylethyl)amine (L^R-H).** To a solution of 1.13 g (7.52 mmol) of 4-*tert*-butylphenol and 1.10 mL (7.52 mmol) of (*R*)-(+)-*N*-α-dimethylbenzylamine in MeOH (50 mL), 0.80 mL (10.64 mmol) of formaldehyde (37% solution in H_2O) was added. The solution was stirred and heated under reflux for 24 h until a crude product precipitated as a white solid. It was collected by filtration, washed with cold methanol and dried *in vacuo* to give L^R-H. Yield 86% (1.92 g, 6.47 mmol).

Anal. Calcd (Found) for $C_{20}H_{27}NO$: C, 80.76 (80.53); H, 9.15 (9.45); N, 4.71 (4.63)%; ESI/MS: 298.2 $[M + 1]^+$; ^{1}H NMR (500 MHz, $CDCl_3$, RT): δ = 11.18 (br, s, 1H, **OH**), 7.39–7.27 (m, **ArH**, 5H), 7.16 (dd, J_{HH} = 8.4, 2.5 Hz, 1H, **ArH**), 6.92 (d, J_{HH} =

2.4 Hz, 1H, **ArH**), 6.75 (d, J_{HH} = 8.4 Hz, 1H, **ArH**), 3.85–3.56 (m, 2H, **N-CH$_2$-Ar**), 3.79 (q, J_{HH} = 6.9 Hz, 1H, **N-CH-Ar**), 2.22 (s, 3H, **N-CH$_3$**), 1.51 (d, J_{HH} = 6.9, 3H, **CH$_3$-CH**), 1.26 (s, 9H, **C(CH$_3$)$_3$**); ^{13}C NMR (75 MHz, $CDCl_3$, RT): δ = 155.7 (**ArC-OH**, 1C), 141.8 (**ArC-C**, 1C), 140.8 (**ArC-CH**, 1C), 128.6 (**ArCH**, 2C), 128.2 (**ArCH**, 2C), 127.7 (**ArCH**, 1C), 125.4 (**ArCH**, 1C), 125.3 (**ArCH**, 1C), 121.2 (**ArC-CH$_2$**, 1C), 115.4 (**ArCH**, 1C), 62.8 (**N-CH-Ar**, 1C), 58.6 (**N-CH$_2$-Ar**, 1C), 37.4 (**N-CH$_3$**, 1C), 34.1 (**C(CH$_3$)$_3$**, 1C), 31.7 (**C(CH$_3$)$_3$**, 3C), 17.5 (**CH$_3$-CH**, 1C).

L^S-H. This compound was prepared in the same manner as described above for L^R-H but (*S*)-(−)-*N*-α-dimethylbenzylamine instead of (*R*)-(+)-*N*-α-dimethylbenzylamine was used.

***N*-[Methyl(2-hydroxy-5-*tert*-butylphenyl)]-*N*-dimethylamine (L^{Me}-H).** To a solution of 1.50 g (10.00 mmol) of 4-*tert*-butylphenol in MeOH (50 mL), dimethylamine (2 M solution in MeOH, 10.00 mmol) and then 1.10 mL (14.63 mmol) of formaldehyde (37% solution in H_2O) were added. The solution was stirred and heated under reflux for 24 h until a crude product precipitated as a white solid. It was collected by filtration, washed with cold methanol and dried *in vacuo* to give L^{Me}-H. Yield 91% (1.89 g, 9.10 mmol). Anal. Calcd (Found) for $C_{13}H_{21}NO$: C, 75.32 (75.12); H, 10.21 (10.65); N, 6.76 (6.82)%; ESI/MS: 208.2 $[M + 1]^+$; ^{1}H NMR (500 MHz, $CDCl_3$, RT): δ = 10.57 (br, s, 1H, **OH**), 7.20 (dd, J_{HH} = 8.5, 2.5 Hz, 1H, **ArH**), 6.97 (d, J_{HH} = 2.4 Hz, 1H, **ArH**), 6.78 (d, J_{HH} = 8.4 Hz, 1H, **ArH**), 3.64 (s, 2H, **N-CH$_2$-Ar**), 2.33 (s, 6H, **N-CH$_3$**), 1.30 (s, 9H, **C(CH$_3$)$_3$**); ^{13}C NMR (75 MHz, $CDCl_3$, RT): δ = 155.7 (**ArC-OH**, 1C), 141.7 (**ArC-C**, 1C), 125.5 (**ArCH**, 1C), 125.2 (**ArCH**, 1C), 121.3 (**ArC-CH$_2$**, 1C), 115.5 (**ArCH**, 1C), 63.5 (**N-CH$_2$-Ar**, 1C), 44.7 (**N-CH$_3$**, 2C), 34.1 (**C(CH$_3$)$_3$**, 1C), 31.7 (**C(CH$_3$)$_3$**, 3C).

[*RR*-Zn]. To a solution of L^R-H (0.59 g, 2.00 mmol) in hexanes (50 mL), $ZnEt_2$ (2 mL, 2.00 mmol) was added dropwise at room temperature. The solution was stirred until a white solid precipitated. It was filtered off, washed with hexanes (10 mL) and dried *in vacuo*. The product was recrystallized from toluene at −15 °C to give a crystalline colourless solid. Yield 77% (0.60 g, 0.77 mmol). Anal. Calcd (Found) for $C_{44}H_{62}N_2O_2Zn_2$: C, 67.60 (67.49); H, 7.99 (8.06); N, 3.58 (3.56)%; ^{1}H NMR (500 MHz, C_6D_6, RT): δ = 7.49 (d, J_{HH} = 7.4 Hz, 2H, ***ArH***, ArH), 7.33 (s, 1H, *ArH*), 7.31 (d, J_{HH} = 8.8 Hz, 1H, **ArH**), 7.27–7.11 (m, 10H, ArH), 7.12 (s, 2H, ***ArH***, *ArH*), 7.08 (d, J_{HH} = 7.6 Hz, 1H, *ArH*), 7.04 (d, J_{HH} = 8.5 Hz, 1H, **ArH**), 6.96 (s, 2H, ***ArH***, ArH), 6.86 (s, 2H, **ArH**, *ArH*), 5.08 (q, J_{HH} = 6.9, 1H, **N-CH-Ar**), 4.94 (s, 1H, *N-CH-Ar*), 4.84 (d, J_{HH} = 11.8 Hz, 1H, ***N-CH$_2$-Ar***), 4.80 (d, J_{HH} = 10.1 Hz, 2H, **N-CH$_2$-Ar**, *N-CH$_2$-Ar*), 4.49 (q, J_{HH} = 6.8 Hz, 1H, ***N-CH-Ar***), 3.95 (s, 2H, N-CH-Ar, N-CH$_2$-Ar), 3.58 (s, 1H, N-CH$_2$-Ar), 3.29 (d, J_{HH} = 11.8 Hz, 1H, ***N-CH$_2$-Ar***), 3.09 (d, J_{HH} = 11.8 Hz, 2H, **N-CH$_2$-Ar**, *N-CH$_2$-Ar*), 2.61 (s, 3H, N-CH$_3$), 2.02 (s, 3H, *N-CH$_3$*), 1.99 (s, 3H, **N-CH$_3$**), 1.92 (s, 3H, ***N-CH$_3$***), 1.75 (d, J_{HH} = 7.5, 3H, *CH$_3$-CH*), 1.68 (d, J_{HH} = 7.5, 3H, **CH$_3$-CH**), 1.66 (d, J_{HH} = 7.5, 3H, ***CH$_3$-CH***), 1.54 (t, J_{HH} = 8.1, 3H, CH$_3$-CH$_2$), 1.46 (s, CH$_3$-CH), 1.38 (t, J_{HH} = 8.1, 3H, **CH$_3$-CH$_2$**), 1.31 (t, J_{HH} = 8.1, 3H, *CH$_3$-CH$_2$*), 1.29 (s, 21H, ***C(CH$_3$)$_3$***, C(CH$_3$)$_3$ ***CH$_3$-CH$_2$***), 1.17 (s, 9H, *C(CH$_3$)$_3$*), 1.16 (s, 9H, **C(CH$_3$)$_3$**), 0.65–0.57 (m, 2H, CH$_3$-CH$_2$), 0.41 (q, J_{HH} = 8.0, 2H, **CH$_3$-CH$_2$**), 0.35 (q, J_{HH} = 8.1, 2H, *CH$_3$-CH$_2$*), 0.32–0.14 (m, 2H, ***CH$_3$-CH$_2$***); ^{13}C NMR (75 MHz, C_6D_6, RT): δ = 161.5 (*ArC-OH*, ArC-OH, 2C), 161.3 (**ArC-OH**, 1C), 161.2 (***ArC-OH***, 1C), 140.6 (ArC-CH$_2$, 4C), 139.1 (***ArC-CH***, 1C), 136.8 (ArC-CH, 1C), 136.5 (*ArC-CH*, 1C), (**ArC-CH**, 1C), 130.6 (**ArCH**, 2C), 130.5 (*ArCH*, ArCH, 4C), 130.1 (***ArCH***, 2C), 128.8 (***ArCH***, 1C), 128.7 (**ArCH**, *ArCH*, ArCH, 3C), 128.5 (**ArCH**, *ArCH*, ***ArCH***, ArCH, 12C), 127.3 (ArCH, 4C), 125.1 (***ArC-CH$_2$***, 1C), 125.0 (**ArC-CH$_2$**, 1C), 124.6 (*ArC-CH$_2$*, 1C), 123.1 (ArC-CH$_2$, 1C), 120.2 (***ArCH***, ArCH, 2C), 119.9 (**ArCH**, *ArCH*, 2C), 65.1 (***N-CH-Ar***, 1C), 64.2 (*N-CH-Ar*, 1C), 64.1 (**N-CH-Ar**, 1C), 62.4 (N-CH-Ar, 1C), 61.7 (*N-CH$_2$-Ar*, 1C), 61.3 (**N-CH$_2$-Ar**, 1C), 60.7 (N-CH$_2$-Ar, 1C), 58.1 (***N-CH$_2$-Ar***, 1C), 38.8 (***N-CH$_3$***, 1C), 36.3 (N-CH$_3$, 1C), 35.1 (*N-CH$_3$*, 1C), 1C), 34.8 (**N-CH$_3$**, 1C), 34.0 (***C(CH$_3$)$_3$***, C(CH$_3$)$_3$, 2C), 33.9 (**C(CH$_3$)$_3$**, *C(CH$_3$)$_3$*, 2C), 31.9 (***C(CH$_3$)$_3$***, C(CH$_3$)$_3$, 31.8 (**C(CH$_3$)$_3$**, *C(CH$_3$)$_3$*, 6C), 20.2 (**CH$_3$-CH-N**, *CH$_3$-CH-N*, CH$_3$-CH-N, 3C), 15.3 (***CH$_3$-CH-N***, 1C), 13.6 (*CH$_3$-CH$_2$*, 1C) 13.5 (**CH$_3$-CH$_2$**, 1C) 13.4 (CH$_3$-CH$_2$, 1C) 13.3 (***CH$_3$-CH$_2$***, 1C), 0.7 (CH$_3$-CH$_2$, 1C), −1.2 (***CH$_3$-CH$_2$***, 1C) −1.6 (*CH$_3$-CH$_2$*, 1C), −1.7 (**CH$_3$-CH$_2$**, 1C).

[*SS*-Zn]. This compound was prepared in the same manner as described above for [*RR*-Zn] but L^S-H instead of L^R-H was used.

[*RS*-Zn]. [*RR*-Zn] (0.78 g, 1.00 mmol) and [*SS*-Zn] (0.78 g, 1.00 mmol) were dissolved in toluene (20 mL) at room temperature. The solution was stirred and concentrated *in vacuo*, then put at −15 °C. After 24 h, the product [*RS*-Zn] was obtained as colourless crystals in 87% yield (1.36 g, 1.74 mmol). Anal. Calcd (Found) for $C_{44}H_{62}N_2O_2Zn_2$: C, 67.60 (67.53); H, 7.99 (8.03); N, 3.58 (3.55)%; ^{1}H NMR (500 MHz, C_6D_6, RT): δ = 7.30 (dd, J_{HH} = 8.4, 2.6 Hz, 2H, **ArH**), 7.25–7.10 (m, 10H, **ArH**), 7.07 (d, J_{HH} = 8.4 Hz, 2H, **ArH**), 6.87 (d, J_{HH} = 2.5 Hz, 2H, **ArH**), 5.06 (q, J_{HH} = 7.0 Hz, 2H, **N-CH-Ar**), 4.86 (d, J_{HH} = 12.0 Hz, 2H, **N-CH$_2$-Ar**), 3.12 (d, J_{HH} = 12.0 Hz, 2H, **N-CH$_2$-Ar**), 1.99 (s, 6H, **N-CH$_3$**), 1.68 (d, J_{HH} = 7.0, 6H, **CH$_3$-CH**), 1.48 (t, J_{HH} = 8.1 Hz, 6H, **CH$_2$-CH$_3$**), 1.15 (s, 18H, **C(CH$_3$)$_3$**), 0.47 (q, J_{HH} = 8.1 Hz, 4H, **CH$_2$-CH$_3$**); ^{13}C NMR (75 MHz, C_6D_6, RT): δ = 161.5 (**ArC-C**, 2C), 140.7 (**ArC-C**, 2C), 136.3 (**ArC-CH**, 2C), 130.6 (**ArCH**, 4C), 128.6 (**ArCH**, 8C), 128.4 (**ArCH**, 2C), 124.9 (**ArC-CH$_2$**, 2C), 119.9 (**ArCH**, 2C), 64.6 (**N-CH-Ar**, 2C), 61.5 (**N-CH$_2$-Ar**, 2C), 35.1 (**N-CH$_3$**, 2C), 33.9 (**C(CH$_3$)$_3$**, 2C), 31.8 (**C(CH$_3$)$_3$**, 6C), 20.0 (**CH$_3$-CH**, 2C), 13.6 (**CH$_2$-CH$_3$**, 2C), −1.5 (**CH$_2$-CH$_3$**, 2C).

[*Cy*-Zn]. This compound was prepared based on a previously published procedure.[4a]

[*RCy*-Zn]. [*RR*-Zn] (0.78 g, 1.00 mmol) and [*Cy*-Zn] (0.74 g, 1.00 mmol) were dissolved in toluene (20 mL) at room temperature. The solution was stirred and concentrated *in vacuo*, then put at −15 °C. After 24 h, the product [*CyR*-Zn] was obtained as a white crystalline powder in 91% yield (1.38 g, 1.82 mmol). Anal. Calcd (Found) for $C_{42}H_{64}N_2O_2Zn_2$: C, 66.40 (66.33); H, 8.49 (8.89); N, 3.69 (3.85)%; ^{1}H NMR (500 MHz, C_6D_6, RT): δ = 7.35 (dd, J_{HH} = 8.3, 2.8 Hz, 1H, ***ArH***), 7.33 (dd, J_{HH} = 8.4, 2.8 Hz, 1H, **ArH**), 7.24–7.12 (m, 5H, **ArH**), 7.12 (d, J_{HH} = 2.7 Hz, 1H, ***ArH***), 7.10 (d, J_{HH} = 8.4 Hz, 1H, ***ArH***), 7.07 (d, J_{HH} = 8.4 Hz, 1H, **ArH**), 6.84 (d, J_{HH} = 2.5 Hz, 1H, **ArH**), 5.07 (q, J_{HH} = 7.0 Hz, 1H, **N-CH-Ar**), 4.82 (d, J_{HH} = 11.9 Hz, 1H, **N-CH$_2$-Ar**), 4.61 (d, J_{HH} = 12.2 Hz, 1H, ***N-CH$_2$-Ar***), 3.37 (d, J_{HH} = 12.0 Hz,

1H, ***N*-CH$_2$-*Ar***), 3.31–3.23 (m, 1H, ***N*-CH**), 3.08 (d, J_{HH} = 12.0 Hz, 1H, **N-CH$_2$-Ar**), 2.26–0.86 (m, 10H, ***CH$_2$***), 1.96 (s, 3H, **N-CH$_3$**), 1.88 (s, 3H, ***N*-CH$_3$**), 1.67 (d, J_{HH} = 7.1, 3H, **CH$_3$-CH**), 1.43 (t, J_{HH} = 8.1 Hz, 3H, **CH$_2$-CH$_3$**), 1.38 (t, J_{HH} = 8.1 Hz, 3H, ***CH$_2$*-CH$_3$**), 1.36 (s, 9H, ***C*(CH$_3$)$_3$**), 1.14 (s, 9H, **C(CH$_3$)$_3$**), 0.44–0.34 (m, 4H, **CH$_2$-CH$_3$**, ***CH$_2$*-CH$_3$**); ^{13}C NMR (75 MHz, C_6D_6, RT): δ = 161.6 (***ArC*-OH**, 1C), 161.5 (**ArC-OH**, 1C), 140.5 (**ArC-C**, 1C), 140.4 (***ArC*-*C***, 1C), 136.3 (**ArC-CH**, 1C), 130.6 (**ArCH**, 2C), 128.7 (***ArCH***, 1C), 128.5 (**ArCH**, 4C), 127.5 (**ArCH**, 1C), 127.3 (***ArCH***, 1C), 125.1 (***ArC*-CH$_2$**, 1C), 124.9 (**ArC-CH$_2$**, 1C), 120.0 (***ArCH***, 2C), 119.9 (**ArCH**, 1C), 64.6 (**N-CH-Ar**, 1C), 64.3 (***N*-CH**, 1C), 61.5 (**N-CH$_2$-Ar**, 1C), 59.7 (***N*-CH$_2$-*Ar***, 1C), 36.0 (***N*-CH$_3$**, 1C), 34.9 (**N-CH$_3$**, 1C), 34.1 (***C*(CH$_3$)$_3$**, 1C), 33.9 (**C(CH$_3$)$_3$**, 1C), 32.0 (***C*(CH$_3$)$_3$**, 3C), 31.8 (**C(CH$_3$)$_3$**, 3C), 26.8 (***CH$_2$***, 2C), 26.4 (***CH$_2$***, 2C), 25.9 (***CH$_2$***, 1C), 20.0 (**CH$_3$-CH**, 1C), 13.7 (***CH$_2$*-CH$_3$**, 1C), 13.4 (**CH$_2$-CH$_3$**, 1C), −1.3 (***CH$_2$*-CH$_3$**, 1C), −1.6 (**CH$_2$-CH$_3$**, 1C).

[*Me*-Zn]. To a solution of L^{Me}-H (0.41 g, 2.00 mmol) in hexanes (50 mL), $ZnEt_2$ (2 mL, 2.00 mmol) was added dropwise at room temperature. The solution was stirred until a white solid precipitated. It was filtered off, washed with hexanes (10 mL) and dried *in vacuo*. The product was recrystallized from toluene at −15 °C to give a crystalline colourless solid. Yield 83% (0.50 g, 0.83 mmol). Anal. Calcd (Found) for $C_{30}H_{50}N_2O_2Zn_2$: C, 59.90 (59.48); H, 8.38 (8.65); N, 4.66 (4.61)%; ^{1}H NMR (500 MHz, C_6D_6, RT) δ = 7.34 (dd, J_{HH} = 8.4, 26 Hz, 2H, **ArH**), 7.01 (d, J_{HH} = 8.3 Hz, 2H, **ArH**), 7.01 (d, J_{HH} = 2.6 Hz, 2H, **ArH**), 4.44 (d, J_{HH} = 11.9 Hz, 2H, **N-CH$_2$-Ar**), 2.70 (d, J_{HH} = 12.0 Hz, 1H, **N-CH$_2$-Ar**), 2.38 (s, 6H, **N-CH$_3$**), 1.79 (s, 6H, **N-CH$_3$**), 1.33 (s, 18H, **C(CH$_3$)$_3$**), 1.26 (t, J_{HH} = 8.1 Hz, 6H, **CH$_2$-CH$_3$**), 0.28 (q, J_{HH} = 8.1 Hz, 4H, **CH$_2$-CH$_3$**).

^{13}C NMR (126 MHz, C_6D_6, RT) δ = 161.4 (**ArC-OH**, 2C), 140.4 (**ArC-C**, 2C), 127.8 (**ArCH**, 2C), 127.4 (**ArCH**, 2C), 124.9 (**ArC-CH$_2$**, 2C), 120.3 (**ArCH**, 2C), 63.7 (**N-CH$_2$-Ar**, 2C), 46.7 (**N-CH$_3$**, 2C), 44.4 (**N-CH$_3$**, 2C), 34.0 (**C(CH$_3$)$_3$**, 2C), 32.0 (**C(CH$_3$)$_3$**, 6C), 13.5 (**CH$_2$-CH$_3$**, 2C), −3.9 (**CH$_2$-CH$_3$**, 2C).

[*RMe*-Zn]. [*RR*-Zn] (0.78 g, 1.00 mmol) and [*Me*-Zn] (0.60 g, 1.00 mmol) were dissolved in toluene (20 mL) at room temperature. The solution was stirred and concentrated *in vacuo*, then put at −15 °C. After 24 h the product [*CyR*-Zn] was obtained as a white crystalline powder in 88% yield (1.22 g, 1.76 mmol). Anal. Calcd (Found) for $C_{37}H_{56}N_2O_2Zn_2$: C, 64.26 (64.51); H, 8.16 (8.22); N, 4.05 (4.07)%; ^{1}H NMR (500 MHz, C_6D_6, RT) δ = 7.33–7.30 (m, 2H, ***ArH***, **ArH**), 7.19–7.10 (m, 5H, **ArH**), 7.08–7.02 (m, 3H, ***ArH***, **ArH**), 6.83 (d, J_{HH} = 2.6 Hz, 1H, **ArH**), 4.90 (q, J_{HH} = 7.0 Hz, 1H, **N-CH-Ar**), 4.71 (d, J_{HH} = 12.0 Hz, 1H, **N-CH$_2$-Ar**), 4.61 (d, J_{HH} = 12.0 Hz, 1H, ***N*-CH$_2$-*Ar***), 3.07 (d, J_{HH} = 12.0 Hz, 1H, **N-CH$_2$-Ar**), 2.70 (d, J_{HH} = 12.2 Hz, 1H, ***N*-CH$_2$-*Ar***), 2.44 (s, 3H, ***N*-CH$_3$**), 1.95 (s, 3H, **N-CH$_3$**), 1.82 (s, 3H, ***N*-CH$_3$**), 1.69 (d, J_{HH} = 7.1 Hz, 3H, **CH$_3$-CH**), 1.40 (t, J_{HH} = 8.1 Hz, 3H, **CH$_2$-CH$_3$**), 1.33 (s, 9H, ***C*(CH$_3$)$_3$**), 1.30 (t, J_{HH} = 8.1 Hz, 3H, ***CH$_2$*-CH$_3$**), 1.16 (s, 9H, **C(CH$_3$)$_3$**), 0.42 (q, J_{HH} = 8.2 Hz, 2H, **CH$_2$-CH$_3$**), 0.31 (q, J_{HH} = 8.1 Hz, 2H, ***CH$_2$*-CH$_3$**). ^{13}C NMR (126 MHz, C_6D_6, RT) δ = 161.6 (**ArC-OH**, 1C), 161.3 (***ArC*-OH**, 1C), 140.6 (**ArC-C**, 1C), 140.4 (***ArC*-*C***, 1C), 136.3 (**ArC-CH**, 1C), 130.5 (**ArCH**, 2C), 128.5 (**ArCH**, 3C), 128.4 (**ArCH**, 1C), 128.0 (***ArCH***, 1C), 127.5 (**ArCH**, 1C), 127.3 (***ArCH***, 1C), 125.2 (**ArC-CH$_2$**, 1C), 124.5 (***ArC*-CH$_2$**, 1C), 120.3 (***ArCH***, 2C), 119.8 (**ArCH**, 1C), 64.6 (**N-CH-Ar**, 1C), 63.6 (***N*-CH$_2$-*Ar***, 1C), 61.7 (**N-CH$_2$-Ar**, 1C), 46.9 (***N*-CH$_3$**, 1C), 44.3 (***N*-CH$_3$**, 1C), 35.5 (**N-CH$_3$**, 1C), 34.1 (***C*(CH$_3$)$_3$**, 1C), 33.9 (**C(CH$_3$)$_3$**, 1C), 32.0 (***C*(CH$_3$)$_3$**, 3C), 31.8 (**C(CH$_3$)$_3$**, 3C), 19.9 (**CH$_3$-CH**, 1C), 13.8 (**CH$_2$-CH$_3$**, 1C), 13.3 (***CH$_2$*-CH$_3$**, 1C), −1.7 (***CH$_2$*-CH$_3$**, 1C), −3.6 (**CH$_2$-CH$_3$**, 1C).

Details of X-ray data collection and reduction

X-ray diffraction data for a suitable crystal of each sample were collected using a KUMA KM4 CCD Saphire or Xcalibur CCD Onyx (see ESI†) with the ω scan technique at 100 K. The data collection and processing utilized the CrysAlis suite of programs.[5] Space groups were determined based on systematic absences and intensity statistics. Lorentz polarization corrections were applied. The structures were solved using direct methods and refined by full-matrix least-squares on F^2. All calculations were performed using the SHELXTL-2013 suite of programs.[6] All non-hydrogen atoms were refined with anisotropic displacement parameters. Hydrogen atom positions were calculated with geometry and not allowed to vary. Thermal ellipsoid plots were prepared with 30% of probability displacements for non-hydrogen atoms, using the Mercury 3.1 program.[7] All data have been deposited with the Cambridge Crystallographic Data Centre, CCDC: 1046690 for ***RR*-Zn**, 1427070 for ***SS*-Zn**, 1046689 for ***RS*-Zn**, 1427071 for ***RCy*-Zn**, and 1434203 for ***SMe*-Zn**.

Computational details

All density functional theory (DFT) calculations were performed with Gaussian 03 program suite.[8] The geometries of the complexes and ligands were optimized (Tables, in the ESI†) using B3LYP density functional theory and the 6-31G** basis sets, implemented in the Gaussian 03 on all atoms.[9,10] The starting geometries of complexes ***RR*-Zn**, ***SS*-Zn**, ***RS*-Zn**, and ***RCy*-Zn** were generated from their crystal structures, whereas the starting geometries of the adequate monomers were derived from their optimized complexes. The structures of all isomers of the calculated complexes were first optimized *in vacuo*. Next, to obtain results more relevant to the experiment, calculations were performed in the presence of a solvent, while using the Polarizable Continuum Model (PCM) as the SCRF method. Frequency calculations confirmed the stationary points to be minimal on PES.

Theoretical diffusion coefficients (D) have been calculated for DFT optimized structures according to the procedure described by us previously.[4a]

Results and discussion

Recently a family of stable aminophenolate zinc homodimers have been synthesized in our group (Scheme 1). Although in the solid state the dimeric structure is clear and determined using X-ray analysis, in solution a mixture of homodimeric

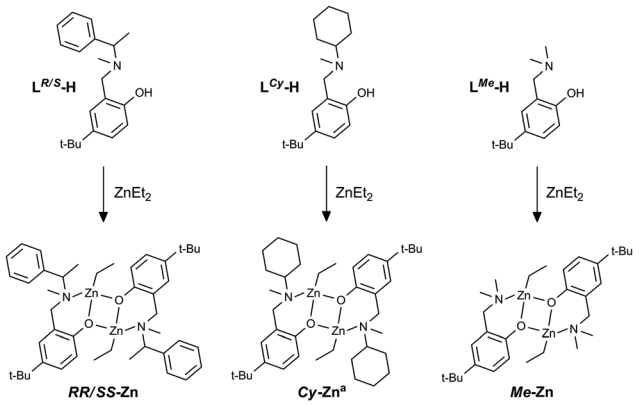

Scheme 1 Synthesis of aminophenolate homodimeric zinc complexes. [a] Previously published.[4a]

isomers has been observed. Therefore, one question is still emerging from the reaction course, whether the equilibrium monomer/dimer or the transformation between the dimers is responsible for the dynamic behavior in the solution, conducted in the mixture of homodimers.

In the **Cy-Zn** complex described earlier (Scheme 1), the asymmetry is due to the arrangement of the prochiral ligand around the metal.[4a] The chiral variant of this type of ligand can probably allow stereo-directing substituents to suppress the number of potential isomers. Therefore, we have modified the nitrogen atom environments by introducing a bulky obstruction containing a single configurationally stable stereogenic centre.

The synthetic procedure for the preparation of chiral ligands is a simple Mannich condensation reaction of chiral amines with phenol and formaldehyde, carried out under reflux with methanol.

These new chiral ligands ($\mathbf{L}^{R}$**–H** and $\mathbf{L}^{S}$**–H**) in the direct reaction with $ZnEt_2$ form aminophenolate zinc complexes ***RR*-Zn** and ***SS*-Zn**, respectively, with ease (Scheme 1). In order to verify the transformation of the potential homodimers, we intermix ***RR*-Zn** and ***SS*-Zn** and we expect only the racemic mixture of the starting complexes. Surprisingly, the symmetric ***RS*-Zn** has been exclusively obtained as the only product.

A lack of these types of well-defined alkyl heterochiral zinc dimers has been observed but some examples are known as inactive reservoirs in a scalemic mixture of precatalysts for asymmetric reactions.[11,12] In this context and in the context of other catalytic applications, the propensity of the formation of these dimers is now of principal interest.

The molecular structures of ***RR*/*SS*-Zn** and ***RS*-Zn** are similar and form classic dimers with four-coordinated zinc centers surrounded by chelating aminophenol ligands, *i.e.* by terminal nitrogen atoms and two bridged oxygen atoms and ethyl groups which are located *trans* to each other. The typical central core rhomboid Zn_2–O_2 is nearly planar and this is a common structural motif in dimeric zinc complexes. All the bond distances and angles between the zinc and O, N and C atoms are typical and comparable with bond lengths and angles observed for similar earlier described complexes.[3,4] The solid state structures of the zinc complexes shown in Fig. 1–3 and Tables S1–2 (see ESI†) summarize the crystal data for the structures of all the zinc complexes reported in this paper.

The ^{1}H NMR spectrum of the homodimeric zinc complexes ***RR*/*SS*-Zn** contains four sets of signals in equivalent ratios (see Fig. 6 and S5†). The spectrum exhibits integrated sharp signals, singlets for amine methyl groups (1.99 and 1.92, ppm) and *tert*-butyl groups (1.29 and 1.16 ppm), and quartets for ethyl groups bonded to the zinc centre at 0.41 and 0.35 ppm. The proton regions, due to the expected methylene doublets and methyl quartets connected with the methylbenzyl substituents bonded to nitrogen atoms, are broadened and less indicative in the spectrum recorded in C_6D_6 solvent at room

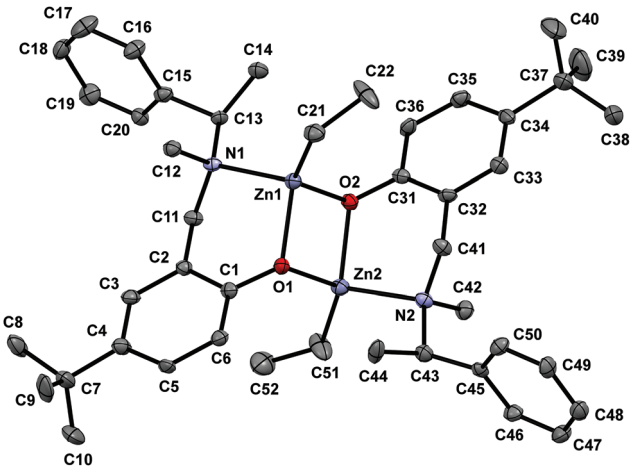

Fig. 1 Molecular structure of ***RR*-Zn**. The thermal ellipsoids are drawn at the 30% probability level. Disorder of *tert*-butyl groups and H atoms are excluded for clarity.

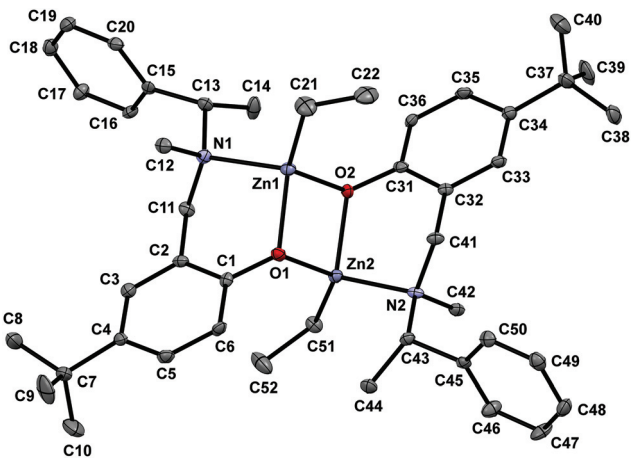

Fig. 2 Molecular structure of ***SS*-Zn**. The thermal ellipsoids are drawn at the 30% probability level. Disorder of *tert*-butyl groups and H atoms are excluded for clarity.

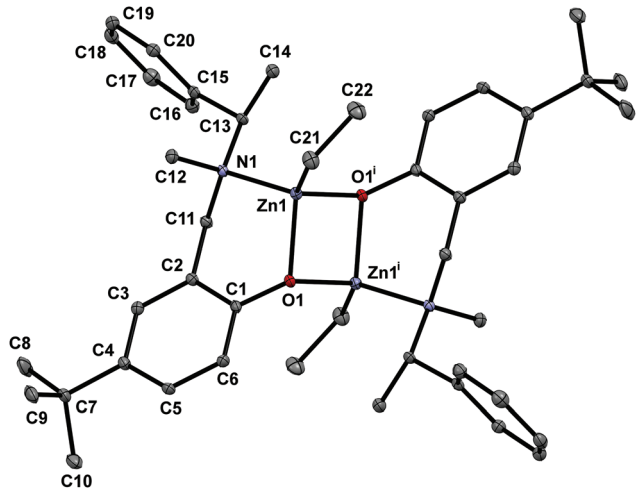

Fig. 3 Molecular structure of ***RS*-Zn**. The thermal ellipsoids are drawn at the 30% probability level, H atoms are excluded for clarity.

temperature. In order to obtain reasonable assignments for this compound, variable temperature NMR studies were conducted. The features in this spectrum are broadened and hence became more complex at lower temperatures (see ESI, Fig. S15†). The variable temperature NMR analysis as well as NOESY are unable to discern whether the intramolecular rearrangements or the monomer/dimer equilibrium (or both) are involved. The DOSY data showed that ***RR*/*SS*-Zn** remain as dimeric structures in solution (see ESI, Table S11†).

During the first stage of the reaction, invisible in NMR, $ZnEt_2$ reacts with appropriate chiral ligands forming coordinately unsaturated monomers, however, next the dimerization occurs stereoselectively. Homochiral dimerization gives several possible isomers characterized by the configuration at the carbon atom (R for L^R or S for L^S, according to the ligands used in the synthesis) which is next amplified at nitrogen and zinc atoms, respectively. The molar ratio of the possible isomers probably depends on the dynamic processes which are supposedly evoked by a stereo-directing group, which leads to the interconversion of the configuration of the nitrogen atoms, while the coordination motif is being built (for the possible isomers obtained by these processes, see Fig. 4 and S23–24†). The consequence of this molecular fitting is that the homodimeric zinc complex is in equilibrium with the corresponding dimeric species in which the central Zn–O–Zn–O rhomboid is intact while the phenol side arm is dangling. The dynamic behaviour in solution may cause broadened resonances for the methylene fragments of the side arms and the methine protons situated on the nitrogen substituents.

When both ***RR*-Zn** and ***SS*-Zn** coexist in solution, the heterochiral combination between them occurs preferentially and leads, among other possibilities, solely to ***RS*-Zn** possessing an S/R configuration at the carbon and nitrogen and a Λ and Δ configuration at the zinc atoms.

The ^{1}H NMR spectrum of ***RS*-Zn** is clear and as anticipated, there is only one set of well-resolved signals, which proved that the two ligands adopted the same coordination mode, consistent with the *meso* structure (Fig. S7†). In contrast to the ^{1}H NMR spectrum of ***RR*-Zn**/***SS*-Zn**, the signals for the ***RS*-Zn** complex could be ascribed exactly to the protons of the methylene group, represented as two doublets at δ = 4.42 and 2.83 ppm; the next quartet of the methyl group bonded to the asymmetric carbon atom, assigned at 4.93, and the signals at δ = 1.04 (triplet) and −0.04 (quartet) correspond to the ethyl

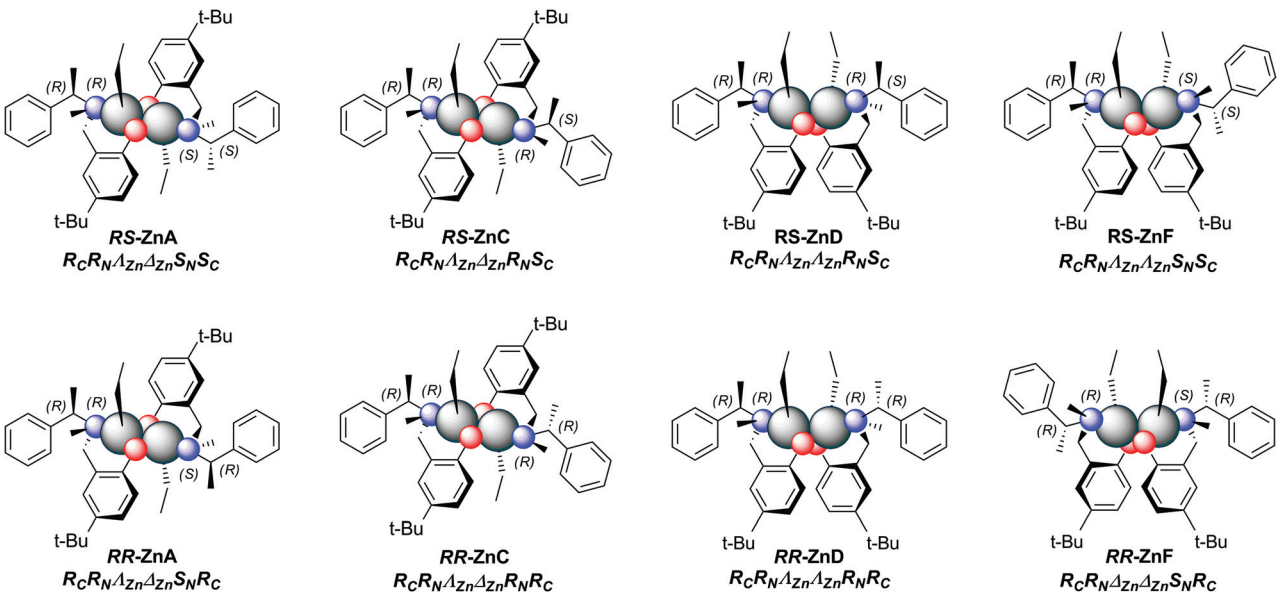

Fig. 4 Schematic structure of the selected heterochiral ***RS*-Zn** and homochiral ***RR*-Zn** isomers.

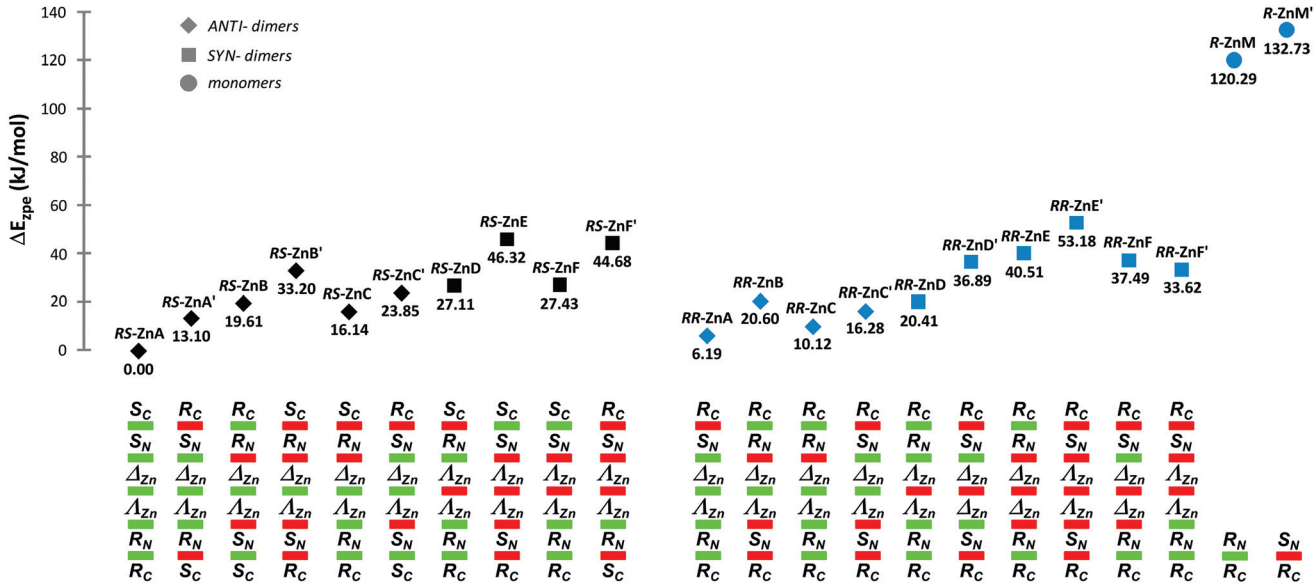

Fig. 5 Relative energies of the ***RS*/*RR*-Zn** isomers in benzene (blue – possible only when one enantiomer of the ligand occurs) and the corresponding molecular codes: green – favorable; red – unfavorable neighborhood of chiral centers.

group bonded to the zinc centre. The pattern of the spectrum is temperature independent (Fig. S16†), thus the ***RS*-Zn** dimer appears to be stable in the solution and this conclusion has been verified by DOSY experiments which additionally suggest stability of the heterodimeric structural motif in solution.

For the purpose of comparing the molecular structure determined using X-ray diffraction and to delineate the possible isomers in the solution, the geometrical parameters and relative energies of both homo- and heterodimeric zinc complexes were investigated by means of DFT calculations at the B3LYP levels while using the 6-31G** basis set (for details see ESI†).

The structural motifs of all generated isomers are shown in Fig. S23–24† (selected in Fig. 6) and their simplified version, indicative of the relations between the neighboring chiral centres is presented in Fig. 5.

Considering the zinc dimers, a full comparison of both homo- and heterochiral dimeric isomers has been achieved. This analysis indicates differences between the *syn*- and *anti*-related conformations of the homo- and heterochiral series. The complexes with ethyl groups arranged *anti* to one another with respect to the Zn–O_2 plane are more favorable compared to the *syn*-structures (Fig. 5).

The theoretically determined energies reveal that the experimentally obtained *anti*-heterodimer ***RS*-Zn** is intrinsically the most stable structure.

In order to decode an experimental NMR spectrum of the chiral homodimer ***RR*-Zn** and to verify which isomers are detectable in solution, theoretical NMR spectra were computed with geometries obtained from DFT studies. The results of this analysis indicated that both the experimental and calculated NMR signals are best matched to isomers with the lowest energy, ***RR*-ZnA** and ***RR*-ZnC**. The ***RR*-ZnC** isomer, proposed by the DFT study possessed agreeable configurations of both carbon and nitrogen atoms (^{1}H NMR signals marked as green and grey, Fig. 6) and is probably the first compound formed during the dimerization process. The transformation of this isomer to the most stable ***RR*-ZnA** isomer (signals marked as red and blue, Fig. 6) is predictable using theoretical calculations.

Based on the experimental and calculated NMR spectra (see Table 1) the homochiral ***RR*-Zn** dimer is a mixture of ***RR*-ZnA** and ***RR*-ZnC** isomers during mutual transformation (Fig. 6). The previous findings from NMR stating that homochiral forms are in a balanced equilibrium are fully reinforced by these DFT calculations.

The final ^{1}H NMR spectra of ***RS*-Zn** contain a single set of sharp peaks at room temperature that is consistent with the structures in solution that are dimeric, or the rapidly equili-

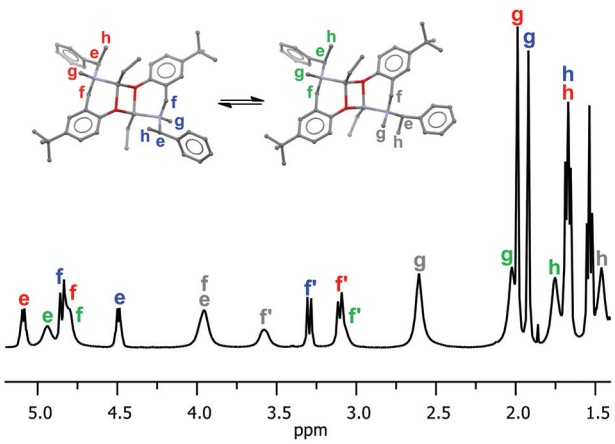

Fig. 6 A fragment of the ^{1}H NMR spectrum of ***RR*-Zn**.

Table 1 Selected ^{1}H NMR chemical shifts for ***RR*-Zn** in benzene-d_6: DFT – calculated for optimized structures, EXP – experimental

			^{1}H NMR chemical shifts	
Isomer	Part		DFT	EXP
RR-ZnA	$R_CR_N\Lambda_{Zn}$	e	4.98	5.08
		f	4.40	4.8
		f′	2.67	3.09
		g	2.18	1.99
		h	1.79	1.68
	$R_CS_N\Delta_{Zn}$	e	4.33	4.49
		f	4.90	4.84
		f′	3.28	3.29
		g	1.96	1.92
		h	2.10	1.66
RR-ZnC	$R_CR_N\Lambda_{Zn}$	e	4.95	4.94
		f	4.63	4.8
		f′	2.73	3.09
		g	2.15	2.02
		h	1.71	1.75
	$R_CR_N\Delta_{Zn}$	e	3.99	3.95
		f	4.18	3.95
		f′	3.15	3.58
		g	2.69	2.61
		h	1.64	1.46

brating mixtures. But the following question may arise: is the monomer the real structure of the intermediate species in this reaction? The experimental and calculated data suggest that the homodimer transformation is a more tenable heterodimerization pathway. Because the origin of the self-sorting process of zinc complexes has remained unclear, the crossover titration experiments in an NMR tube have been undertaken (Fig. 7). First, to ***RR*-Zn** solution in C_6D_6, ***SS*-Zn** has been added in the sequence of 1/0.5 and 1/1 molar ratio. The racemic mixture of ***RR*-Zn** and ***SS*-Zn** should show an unchanged pattern in the

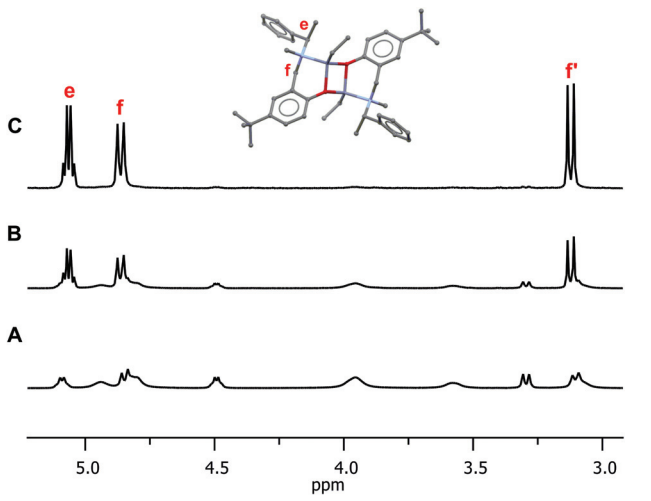

Fig. 7 The monitoring of the reaction between the chiral dimers by ^{1}H NMR. ***RR*-Zn** and ***SS*-Zn** in the following molar ratios: 1/0 (A), 1/0.5 (B), and 1/1 (C).

NMR spectra, the absence of additional resonances potentially rules out the exclusive formation of heterodimeric species, in this example ***RS*-Zn**. But here, during the titration experiment, we have observed the formation process of ***RS*-Zn** (Fig. 7B), although the NMR spectrum of the ***RS*-Zn** complex (Fig. 7C) is nearly identical to one of the signal sets corresponding to the starting homochiral dimer (Fig. 7A). The reaction of the potentially formed monomers that later statistically dimerized is clear when in the NMR spectrum the presence of the signals corresponding to the homo- and heterodimeric species could be observed.[3a] However, no monomeric species have been detected as an independent entity, even at low temperatures.

The monomeric forms seem to be absent which was additionally supported by the highest energy of the generated monomeric species obtained by DFT calculations (Fig. 5).

This preferred interaction between the components of opposite chirality leads to the spontaneous selection of enantiomers to form a favored heterochiral product (Scheme 2).

In the chiral self-sorting system discussed here, the pairs of enantiomers differ only in their relative spatial orientation derived from their opposite chirality, therefore, typical geometrical factors do not exhibit an overwhelming preponderance. However, a high tendency to form stable dimers and the flexibility of the amine arm of the ligands are undoubtedly additional molecular codes that enable particular homodimers to recognize each other. Therefore, we have focused on the study of geometrical complementarity together with chiral constraint of aminophenolate ligands over the reaction course. The stable homodimer ***Cy*-Zn** appears to be a suitable target for such investigation because it combines a similar shape to ***RR*-Zn** and the possibility to arrange suitable chirality on nitrogen atoms. The reaction between ***RR*-Zn** and ***Cy*-Zn** gives an exclusively heterodimeric complex, ***RCy*-Zn**, with the expected structural motif containing a Zn_2–O_2 rhomboid and each of the zinc atoms being surrounded by different aminophenolate ligands.

Distinctive ^{1}H NMR signals of ***RCy*-Zn** include the methylene backbone and methine protons at 4.82, 3.08 and 5.07 corresponding to the chiral ligand bonded to the zinc atom. In addition, the doublets of the methylene protons of the L^{Cy} fragment at 4.61 and 3.37 ppm are visible (see Fig. 8 and S9†).

The chiral clips of the L^R fragment constrain the appropriate opposite configuration on the nitrogen atoms of the L^{Cy} part to form the stable heterodimer ***RCy*-Zn**.

Accordingly, to ensure fidelity of the self-sorting process, a sufficient complex for the reaction with chiral ***RR*-Zn** could be the stable achiral homodimer. For this purpose, we have prepared a suitable ***Me*-Zn** homodimer with appropriate aminophenolate ligands containing nitrogen atoms with two methyl substituents. As a consequence, in the one pot reaction between ***Me*-Zn** and chiral ***RR*-Zn**, the new heterodimer ***RMe*-Zn** has been formed.

The NMR spectrum of this heterodimer shows signals belonging to the appropriate ligands coordinated to zinc atoms. The methylene and methine protons are distinguished in the chiral fragment doublets at 4.70 and 3.07 and a quartet

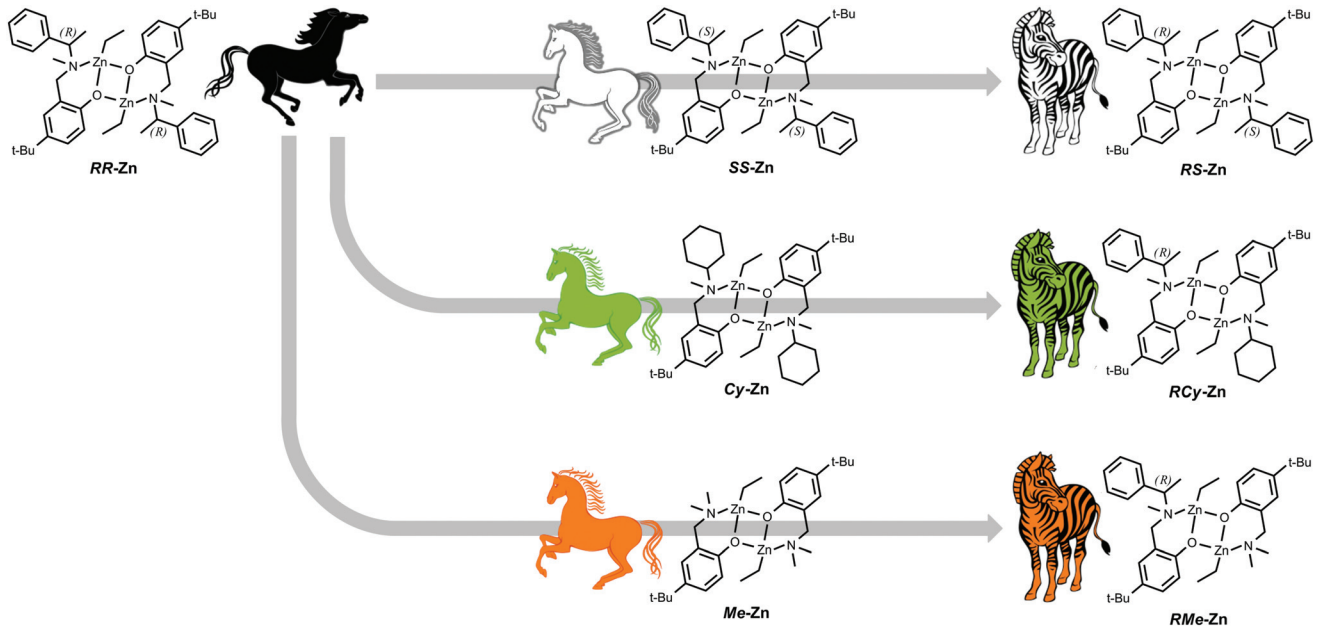

Scheme 2 Synthesis of aminophenolate heterodimeric zinc complexes – the zebra reaction.

at 4.90 ppm, respectively, and the new methylene signals at 4.61 and 2.70 ppm. (see Fig. 9 and S13†).

The detailed information describing the structural data in solution is in the Experimental section and ESI, Fig. S9–12, S20, 22 and Tables S8, 10†, while the molecular structures of ***RCy*-Zn** and ***SMe*-Zn** are presented in Fig. 10 and 11 (for details see ESI: Tables S1–2†).

The selective formation of the heterodimeric zinc complexes has been carried out in a direct reaction between the chiral homodimer and the chiral/achiral ones. What is more, in the reaction in the absence of a chiral substrate, in our example: Me–Zn and Cy–Zn give the mixture of homo-/heterodimers.

Although the X-ray analysis correlates with the structures in the solution provided by NMR, the DFT study offers additional information to clarify the heterodimerization pathway in the "zebra reaction". The chiral clips C_RN_RZn during homochiral dimerization form a mixture of isomers but two of them which undergo dynamic behavior arise from the competition between chiral and geometrical codes; ***RR*-ZnA** $(R_CR_N\Lambda_{Zn}\Delta_{Zn}S_NR_C)$ and ***RR*-ZnC** $(R_CR_N\Lambda_{Zn}\Delta_{Zn}R_NR_C)$,

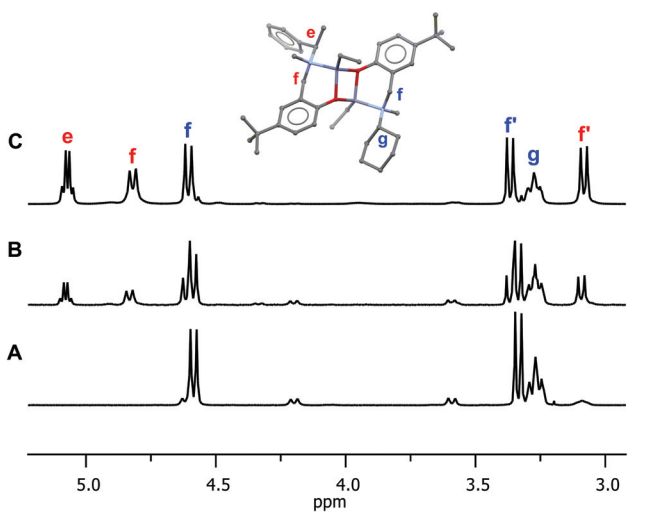

Fig. 8 The monitoring of the reaction between ***RR*-Zn** and ***Cy*-Zn** by ^{1}H NMR. ***Cy*-Zn** and ***RR*-Zn** in the following molar ratios: 1/0 (A), 1/0.5 (B), 1/1 (C).

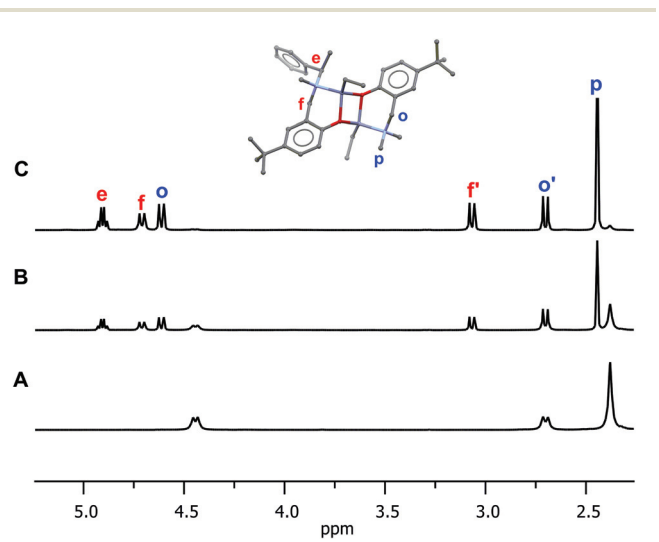

Fig. 9 Monitoring the reaction between ***RR*-Zn** and ***Me*-Zn** by ^{1}H NMR. ***Me*-Zn** and ***RR*-Zn** in the following molar ratios: 1/0 (A), 1/0.5 (B), 1/1 (C).

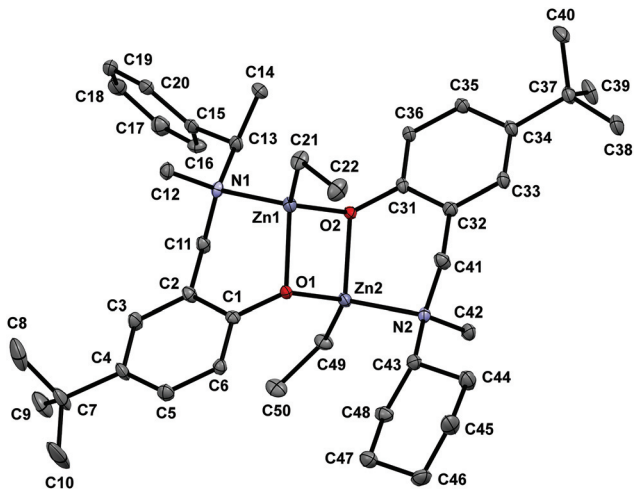

Fig. 10 Molecular structure of ***RCy*-Zn**. The thermal ellipsoids are drawn at the 30% probability level. Disorder of the *tert*-butyl group and H atoms are excluded for clarity.

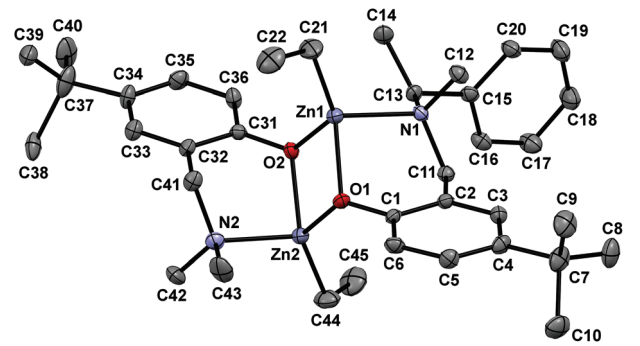

Fig. 11 Molecular structure of ***SMe*-Zn**. The thermal ellipsoids are drawn at the 30% probability level. Disorder of the *tert*-butyl groups and H atoms are excluded for clarity.

respectively. Destabilization of one ligand arm by changing the nitrogen atom configuration seems to be the driving force of the reaction between the appropriate dimers (Fig. 12).

The "black horse" ***RR*-Zn** can gallop with the "white" one (opposite chirality ***SS*-Zn**) and form the "white and black zebra", ***RS*-Zn**, presenting the molecular code $R_CR_N\Lambda_{Zn}\Delta_{Zn}S_NS_C$. While when the zinc dimer with the prochiral ligand L^{Cy} meets the "black horse", it forms ***RCy*-Zn** ($R_CR_N\Lambda_{Zn}\Delta_{Zn}S_N$) easily, and the best is to match with the flexible ***Me*-Zn** which gets transformed into ***RMe*-Zn** ($R_CR_N\Lambda_{Zn}\Delta_{Zn}$). What is important to note is that the two chiral clips, although uncomfortable during the formation of the homodimers, are crucial for heterodimers, because the "zebras" (***RS*-Zn**, ***RCy*-Zn** and ***RMe*-Zn**) with stable codes are unable to react with each other. This clearly shows the power of chemistry, because nobody has seen a zebra as the offspring of two horses but chemistry facilitates the magic.

The new examples with more detailed analysis of the key structural features, responsible for the chiral-directed self-sorting process and the application of these zinc complexes in catalysis, constitute the subject of our intensive research at the moment. The findings of our research will be published in a different paper soon.

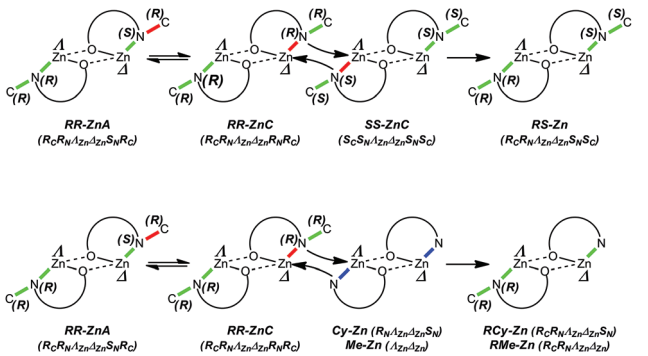

Fig. 12 The proposed mechanism of heterodimer formation. / – favorable; / – unfavorable / – switchable relation of chiral centers.

Conclusions

The recipe for zinc heterodimers is simple: homodimers, which are more stable than their monomers (confirmed by a DFT study during the design process) and one of the homodimers with a chiral clip can form unique heterodimers containing zinc atoms bearing different ligands.

Acknowledgements

The authors gratefully acknowledge the National Science Centre in Poland (Grant NN 204 200640), the Wrocław Centre for Networking and Supercomputing (http://www.wcss.wroc.pl), and EU under the European Social Found (project Academy of development as the key to strengthen human resources of the Polish economy) for the support of this research.

Notes and references

1 See for examples: (*a*) G. Consiglio, S. Failla, P. Finocchiaro, I. P. Oliveri, R. Purrello and S. Di Bella, *Inorg. Chem.*, 2010, **49**, 5134; (*b*) A. W. Kleij, *Dalton Trans.*, 2009, 4635; (*c*) K. Zhang, H. Qian, L. Zhang and W. Huan, *Inorg. Chem.*, 2015, **54**, 675; (*d*) I. P. Oliveri, G. Malandrino and S. Di Bella, *Inorg. Chem.*, 2014, **53**, 9771; (*e*) P. Roy, K. Dhara, M. Manassero, J. Ratha and P. Banerjee, *Inorg. Chem.*, 2007, **46**, 6405; (*f*) I. Giannicchi, R. Brissos, D. Ramos, J. de Lapuente, J. C. Lima, A. D. Cort and L. Rodríguez, *Inorg. Chem.*, 2013, **52**, 9245; (*g*) Y. Sarazin and J.-F. Carpentier, *Chem. Rev.*, 2015, **115**, 3564; (*h*) M. I. Childers, J. M. Longo, N. J. V. Zee, A. M. LaPointe and G. W. Coates, *Chem. Rev.*, 2014, **114**, 8129.

2 (*a*) B. M. Chamberlain, M. Cheng, D. R. Moore, T. M. Ovitt, E. B. Lobovsky and G. W. Coates, *J. Am. Chem. Soc.*, 2001, **123**, 3229; (*b*) M. H. Chisholm, J. C. Huffman and K. Phomphrai, *Dalton Trans.*, 2001, **3**, 222; (*c*) A. P. Dove, V. C. Gibson, E. L. Marshall, A. J. P. White and D. J. Wiliams, *Dalton Trans.*, 2004, 570; (*d*) F. Drouin, P. O. Ogadinma, T. J. J. Whitehornr, R. E. Prud'homme and F. Schaper, *Organometallics*, 2010, 29; (*e*) M. H. Chisholm, N. W. Eilerts, J. C. Huffman, S. S. Iyer, M. Pacold and K. Phomphrai, *J. Am. Chem. Soc.*, 2000, **122**, 11845; (*f*) H. Y. Chen, H. Y. Tang and C. C. Lin, *Macromolecules*, 2006, **39**, 3745; (*g*) Z. Zheng, G. Zhao, R. Fablet, M. Bouyahyi, C. M. Thomas, T. Roisnel, O. Casagrande Jr. and J.-F. Carpentier, *New J. Chem.*, 2008, **32**, 2279; (*h*) G. Labourdette, D. J. Lee, B. O. Patrick, M. B. Ezhova and P. Mehrkhodavandi, *Organometallics*, 2009, **28**, 1309; (*i*) V. Poirier, T. Roisnel, J.-F. Carpentier and J. Sarazin, *Dalton Trans.*, 2011, **40**, 523.

3 (*a*) C. K. Williams, L. E. Choi, S. K. Breyfogle, W. Nam, V. G. Young Jr., M. A. Hillmyer and W. B. Tolman, *J. Am. Chem. Soc.*, 2003, **125**, 11350; (*b*) N. Ikpo, L. N. Saunders, J. L. Walsh, J. M. B. Smith, L. N. Dawe and F. M. Kerton, *Eur. J. Inorg. Chem.*, 2011, **35**, 5347; (*c*) J. D. Farwell, P. B. Hitchcock, M. F. Lappert, G. A. Luinstra, A. V. Protchenko and X.-H. Wei, *J. Organomet. Chem.*, 2008, **693**, 1861; (*d*) S. Groysman, E. Sergeeva, I. Goldberg and M. Kol, *Eur. J. Inorg. Chem.*, 2006, **14**, 2739; (*e*) V. Poirier, T. Roisnel, J.-F. Carpentier and Y. Sarazin, *Dalton Trans.*, 2009, 9820.

4 (*a*) D. Jędrzkiewicz, J. Ejfler, N. Gulia, Ł. John and S. Szafert, *Dalton Trans.*, 2015, **44**, 13700; (*b*) J. Ejfler, S. Szafert, K. Mierzwicki, L. B. Jerzykiewicz and P. Sobota, *Dalton Trans.*, 2008, 6556.

5 *CrysAlisRED Software*, Oxford Diffraction, Wrocław, Poland, 1995–2004.

6 G. M. Sheldrick, *Acta Crystallogr., Sect. A: Fundam. Crystallogr.*, 2008, **64**, 112.

7 C. F. Macrae, I. J. Bruna, J. A. Chisholm, P. R. Edgington, P. Mccabe, E. Pidcock, L. Rodriguez-Monge, R. Taylor, J. van de Streek and P. A. Wood, *J. Appl. Crystallogr.*, 2008, **41**, 466.

8 M. J. Frisch, G. W. Trucks, H. B. Schlegel, G. E. Scuseria, M. A. Robb, J. R. Cheeseman, G. Scalmani, V. Barone, B. Mennucci, G. A. Petersson, H. Nakatsuji, M. Caricato, X. Li, H. P. Hratchian, A. F. Izmaylov, J. Bloino, G. Zheng, J. L. Sonnenberg, M. Hada, M. Ehara, K. Toyota, R. Fukuda, J. Hasegawa, M. Ishida, T. Nakajima, Y. Honda, O. Kitao, H. Nakai, T. Vreven, J. A. Montgomery Jr., J. E. Peralta, F. Ogliaro, M. Bearpark, J. J. Heyd, E. Brothers, K. N. Kudin, V. N. Staroverov, T. Keith, R. Kobayashi, J. Normand, K. Raghavachari, A. Rendell, J. C. Burant, S. S. Iyengar, J. Tomasi, M. Cossi, N. Rega, J. M. Millam, M. Klene, J. E. Knox, J. B. Cross, V. Bakken, C. Adamo, J. Jaramillo, R. Gomperts, R. E. Stratmann, O. Yazyev, A. J. Austin, R. Cammi, C. Pomelli, J. W. Ochterski, R. L. Martin, K. Morokuma, V. G. Zakrzewski, G. A. Voth, P. Salvador, J. J. Dannenberg, S. Dapprich, A. D. Daniels, O. Farkas, J. B. Foresman, J. V. Ortiz, J. Cioslowski and D. J. Fox, *Gaussian 09 (Revision B.01)*, Gaussian, Inc., Wallingford CT, 2010.

9 A. D. Becke, *J. Chem. Phys.*, 1993, **98**, 5648.

10 C. Lee, W. Yang and R. G. Parr, *Phys. Rev. B: Condens. Matter*, 1988, **37**, 785.

11 (*a*) H. S. Jena and V. Manivannan, *Inorg. Chim. Acta*, 2013, **394**, 210; (*b*) H. S. Jena, *RSC Adv.*, 2014, **4**, 3028.

12 For selected examples, see: (*a*) M. Steigelmann, Y. Nisar, F. Rominger and B. Goldfuss, *Chem. – Eur. J.*, 2002, **8**, 5211; (*b*) L. Schiaffino and G. Ercolani, *Angew. Chem., Int. Ed.*, 2008, **120**, 6938; (*c*) J. Klankermayer, I. D. Gridnev and J. M. Brown, *Chem. Commun.*, 2007, 3151.

